Proc. Indian natn Sci. Acad., 55, A, No. 6, 1989, pp. 871–885.

A BOUNDARY LAYER MODEL FOR THE ANDAMAN ISLANDS

SARAT C KAR AND N RAMANATHAN

Centre for Atmospheric Sciences, Indian Institute of Technology, New Delhi-110016, India

(*Received 21 November 1988; Accepted 4 April 1989*)

The boundary layer characteristics over the Andaman Islands in the Indian Ocean on a clear day in April have been computed by a two-dimensional hydrostatic mesoscale model. This includes parameterisation of soil and vegetation. The influence of soil moisture and vegetation cover on the flow in the boundary layer was evaluated. It is found that a decrease in soil moisture, and an increase in vegetation cover, enhance the heat transfer to the atmosphere which, in turn, alters the boundary layer characteristics. The simulated results are compared with actual observations.

Key Words : Air Flow Over Island; Planetary Boundary Layer; Vegetation; Soil Moisture

INTRODUCTION

MANY atmospheric models have shown the importance of including a planetary boundary layer (PBL) for obtaining better forecasts. The exchange of heat, momentum and moisture between the ground and the overlying circulation is through a PBL. For large scale numerical weather prediction, the exchange of energy between the PBL and the atmosphere above may be more important than the details within the PBL. But, in a study of mesoscale phenomena, such as sea/land breeze, detailed information on the PBL is required.

Earlier mesoscale studies had some limitations: neglect of topography, inadequate parameterisation of subgrid scale processes, linearistion of the governing equations, a constant PBL depth or the neglect or radiation for calculating the surface temperature. The importance of these factors needs to be hardly stressed. A hydrostatic three dimensional primitive equation model in a terrain following coordinate system with boundary layer parameterisation has been developed.[1] Numerous applications of this model in the University of Virginia to the study of mesoscale circulations have been reported in recent literature.

This model provides realistic simulations of the sea/land breeze over a tropical island, namely, the Andaman islands of the Indian ocean (12 °N, 93 °E).[2] But the earlier study by us revealed an overestimation of the wind speed at lower levels during the day. These discrepancies are attributed to inadequate representation of physical effects, such as, the forest coverage, ground albedo and soil moisture variations.

Several investigators[3–7] have shown the importance of including soil chracteristics and vegetation in a numerical model. But, we found that the combined

effect of soil moisture and vegetation cover was not considered. In the present work, the authors wish to examine soil moisture changes and the vegetation cover on the flow pattern over the island. For simplicity, a two-dimensional (2D) version of the model developed in the University of Virginia for simulation has been adapted. The 2D model includes advection and changes of the dependent variables along a horizontal (x) and verical (z) axis.

The Simulated Region

The Andaman island chain in the Bay of Bengal has an average width of 25km and receives a rainfall of about 300cm from both the summer and winter monsoons. Most of its terrain has an elevation below 200m, with a few peaks above 300m. The principal soil type is loamy sand. Bamboo and teak wood forests cover nearly 86 per cent of the total area. A geographical map of the island with the terrain contours is shown in Fig 1.

The Numerical Model

The model used for the present work is the one used in our our earlier work.[2] Here, we will only briefly mention the salient features. The model uses a terrain following vertical coordinate (z^*) of the type

$$Z^* = \bar{S}\left(\frac{Z - Z_g}{S - Z_g}\right), \qquad \text{...(i)}$$

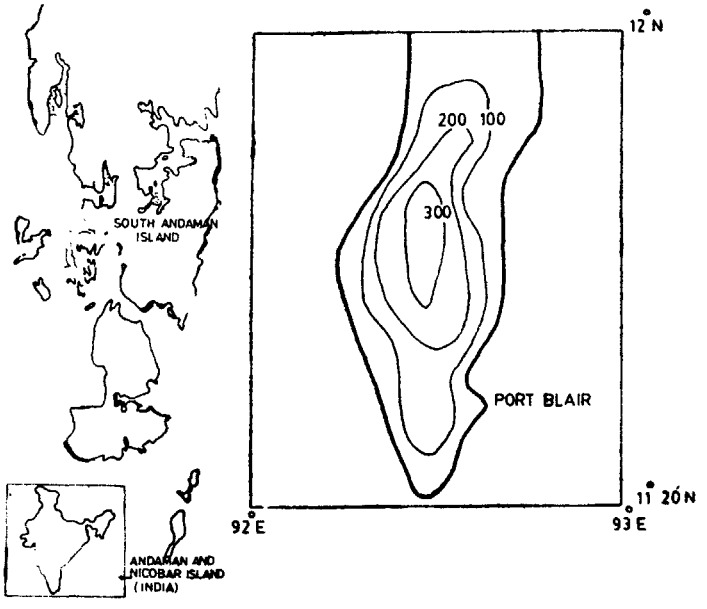

Fig 1 A geographical map of south Andman island (smoothed) with terrain contours. (not to scale; small numbers indicate the terrain elevation in meters above sea level)

where Z_g is the ground elevation, S is the instantaneous value of the material surface top, which changes with time from an initial value of $\bar{S}$. This primitive equation model assumes hydrostatic motion and a first order closure scheme (K-theory) is used to specify the subgrid scale processes. The vertical turbulent exchange coefficients for momentum, heat and moisture were calculated as functions of atmospheric stability using the Monin-Obukov similarity theory. The horizontal turbulence exchange was suppressed by a low pass filter, which removes two grid-length waves. The atmospheric heating/cooling due to radiative flux divergence was also included. The land surface temperature was calculated by a surface energy balance equation which balances the incoming solar radiation with the outgoing terrestrial radiation and turbulent heat fluxes. This model has been well documented in the literature;[1,2,8,9] Therefore, the mathematical details are omitted. A brief description of the features in which the present study differs from the earlier one[2] is described below :

In an earlier work, the authors had assumed bare dry soil of constant wetness and albedo as the lower boundary. A slab model was used in which the heat conduction from lower side of the soil layer was neglected. Evaporation from the soil was not considered in our work. As discussed earlier, about 86 per cent of the land area in the Andamans are covered by forest. So the neglect of vegetation in our earlier study grossly distorted the simulated results. For studying the land/sea breeze, as in the present work, the soil and vegetation characteristics could modify the surface energy balance and, in turn, the land surface temperature. The main objective was to study this aspect.

Soil Parameterisation Scheme

A layered soil parameterisation scheme[10] is used in which the soil temperature (T_s) and soil moisture (η) within the soil layer were computed using time-dependent equations with only vertical diffusion.

$$C \frac{\partial T_s}{\partial t} = \frac{\partial}{\partial z}\left(\lambda \frac{\partial T_s}{\partial z} \right) \qquad ...(2)$$

and

$$\rho_w \frac{\partial \eta}{\partial t} = \frac{\partial W_s}{\partial z} . \qquad ...(3)$$

The volumetric heat capacity C is

$$C = (1 - \eta_s) C_i + \eta . \qquad ...(4)$$

Here, η is the volumetric moisture content, the amount of moisture in cm^3 per unit cubic volume of the moist soil, and η_s is its saturation value, C_i is the dry volumetric heat capacity for soil of type i. The thermal conductivity λ (cal/sec/cm/°C) was related to the available soil moisture and the moisture potential of the soil. The latter is expressed by ψ. It is the suction pressure required to extract water from the soil, ρ_w is the density of liquid water (gm cm^{-3}), W_s is the moisture flux in the soil which is related to the hydraulic conductivity (K_η) and the vertical gradient of Ψ within the soil.

The specific humidity, and the albedo at the surface was expressed as a function of soil wetness. The constants used in the formulation depend on the type of soil. They were specified in the beginning. By assuming continuity across the air-soil interface, a system of governing equations[10] was solved to obtain the surface variables at each time step.

Parameterisation of Vegetation

The authors followed a bulk parameterisation scheme,[3] where the vegetation canopy was considered to be a large leaf covering a fraction (σ_f) of the grid interval (Δx). This single layer canopy acts as an elevated surface intercepting both the short and long wave radiation and limits long wave radiation along with sensible and latent heat. The presence of foliage also affects the solar radiation reaching the ground by shading. In a modified method, the energy fluxes beneath the canopy and for bare ground were calculated separately[4] (Fig. 2).

An expression for energy balance was applied to the canopy to compute the foliage temperature (T_f). The canopy heat storage was assumed to be negligible. This is expressed by

$$\sigma_f(R_s(1 - a_f - a_n) + R_{L\epsilon_f} + (R_2 - R_1)] + H_f + LE_f = 0 \qquad ...(5)$$

In the above equation, the shielding factor σ_f is the fractional shading of a grid cell by vegetation. The incident solar radiation R_s is diminished by a plant albedo (a_f) and the solar zenith angle factor a_n. R_L is the incident long wave radiation from the atmosphere. The outgoing long wave radiation (R_1) and (R_2) was expressed by[9]

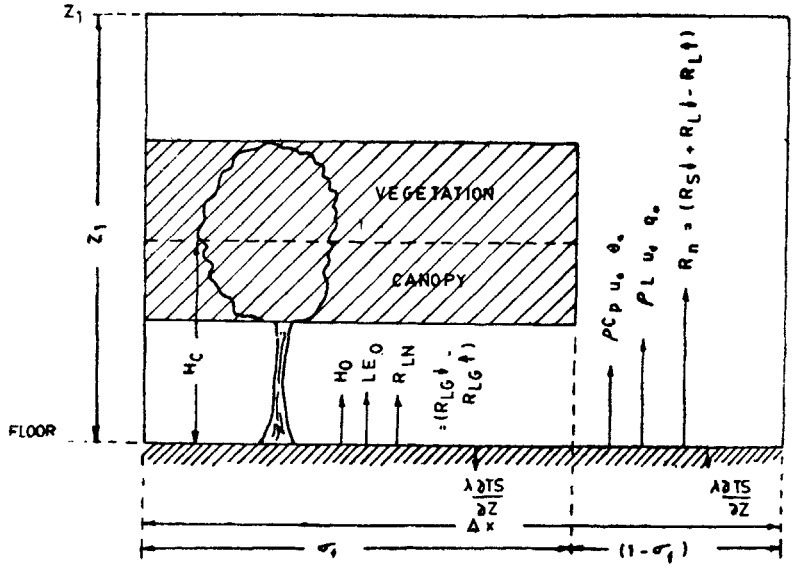

FIG 2 A schematic illustration of the radiative fluxes with vegetation conopy in a grid interval (Δx). Symbols are defined in the text.

$$R_1 = \left[\frac{\epsilon_f + 2\,\epsilon_g - \epsilon_f\,\epsilon_g}{\epsilon_f + \epsilon_g - \epsilon_f\,\epsilon_g}\right] \epsilon_f\,\sigma\,T_f^4 \qquad \ldots(6)$$

$$R_2 = \left[\frac{\epsilon_f\,\epsilon_g}{\epsilon_f + \epsilon_g - \epsilon_f\,\epsilon_g}\right] \sigma\,T_g^4 \qquad \ldots(7)$$

The sensible heat flux (H_f) from the leaves was computed by the equation

$$H_f = 1.1\,LAI\,[\rho\,C_p\,u_{af}\,C_f(T_{af} - T_f)]/\pi. \qquad \ldots(8)$$

The total moisture flux LE_f (evaporation + transpiration) from the leaves is given by

$$LE_f = LAI\,L\,\rho\,f'\,C_f\,u_{af}\,(q_{af} - q_s(T_f)) \qquad \ldots(9)$$

These equations incorporate : (*i*) albedo (a_f) and (*ii*) surface resistance. The factor 1.1 accounts for the stems, trunks and branches which exchange heat, but do not transpire. These equations use : the vegetation characteristics, such as the albedo (a_f), emissivity of the foliage (ϵ_f), leaf area index (LAI), surface resistance (r_c), the wind speed within the canopy (u_{af}), fractional evapotranspiration (f'), transfer coeffieient (C_f), air temperature at the foliage height (T_{af}), the specific humidity of the air at the foliage height (q_{af}) and the saturation specific humidity at the foliage temperature is ($q_s(T_f)$).[3,9]

Over bare ground without vegetation, the surface temperature was computed from the surface energy balance equation[2]

$$R_n + \rho L\,u_* q_* + \rho C_p u_* \Theta_* - \lambda\,\frac{\partial T_s}{\partial z} = 0, \qquad \ldots(10)$$

where R_n is the net radiation flux at the surface, the second and third terms are turbulent latent and sensible heat fluxes respectively, while the last term denotes the soil heat flux. The friction velocity (u_*), temperature (Θ_*) and humidity (q_*) are calculated as functions of stability of the atmosphere. To consider the effect of vegetation, this equation was modified to

$$(1 - \sigma_f)\,(R_n + \rho C_p u_* \Theta_* + \rho L u_* q_*) + \sigma_f(H_o + LE_o + R_{LN}) - \lambda\,\frac{\partial T_s}{\partial z} = 0 \qquad \ldots(11)$$

where $\sigma_f = 0$ denotes a bare soil without vegetations; $\sigma_f = 1$, full coverage by vegetation.

The first terms in parenthesis apply to bare gound while the second group of terms, which appears with σ_f, refer to the fluxes beneath the canopy. The last term denotes the soil heat flux, H_o, LE_o and R_{LN} represent the sensible, latent heat fluxes and net long wave radiation beneath vegetation canopy respectively. These are explained in Fig 2. R_{LN} is computed in terms of foliage temperature (T_f) and the temperature of ground (T_g). The symbols are defined in an appendix.

Surface sensible and latent heat fluxes beneath the canopy were computed by

$$H_o = \rho C_p C_g u_{af}\,(T_{af} - T_g)/\pi \qquad \ldots(12)$$

$$LE_o = \rho L C_g u_{af}\,(q_{af} - q_g) \qquad \ldots(13)$$

The friction velocity, temperature and specific humidity (u_*, θ_*, q_*) were obtained with an average weightage for bare soil and vegetation coverage fraction (σ_f). Surface and foliage temperatures were obtained by solving the respective energy budget equations using a Newton-Raphson iterative technique.[9]

Boundary and Initial Conditions

Boundary Conditions

At the lower boundary,

$$u = v = w^* = 0 \text{ at } z^* = 0 \text{ or } z^* = d.$$

The former corresponds to bare ground, while the latter is for ground with vegetation. d stands for the displacement height.

At the top $z^* = \bar{S} = 7.5$km, $u = u_g$, $v = v_g$ $w^* = 0_9$ $\theta(\bar{S})$ and $q(\bar{S})$ are constants.

At the lateral boundaries ($x = 0$ and $x = L_1$) the boundary conditions make the gradient of the model parameters vanish. We write

$$W^* = \frac{\partial}{\partial x}(s, u, v, q, \theta, \pi, z_g) = 0 \text{ at } x = 0 \text{ and } x = L_i \qquad ...(15)$$

Input Data

Little is known about the energy exchange between synoptic and local circulations. Consequently, to study the energy exchange between the islands and large scale flow, data were considered on days when there were no large scale synoptic disturbances. Days with no precipitation also were considered. One such day was April 1, 1969.

The initial synoptic data, shown in Fig 3 and Table I, were obtained from the Indian daily weather report published by the India Meterological Department. At the start of the simulation, the synoptic temperature, velocity and specific humidity profiles along with profiles of soil temperature were specified from the Port Blair observations. The soil type (loamy sand), the forest type (bamboo/teak) and forest coverage (86 per cent) were taken from an *Atlas of Agricultural Resources of India* (1980). The soil characteristics[11] are given in Table II, while the vegetation characteristics are provided in Table III. The albedo was taken to be 0.15 for vegetation corresponding to a tropical forest.[12] The leaf area index (LAI) was calculated by the relation $LAI = 7\sigma_f$. The stomatal resistance (r_s) of the foliage was taken to be 8 scm^{-1}, which yields a surface resistance of $r_c = r_s/LAI$ of 1.3s cm^{-1}. This value is in agreement with earlier results[13] where r_c for tropical forests was found to vary between 1 to 3s cm^{-1}. Tne observed soil moisture (per cent by volume) variations in forest areas ranged from 8.7 per cent to 4.7 per cent.[14] In our simulation, we have adopted the soil moisture to be within its field capacity, but above the wilting point. In addition the following parameters were initially specified : (1) surface drag coefficient (C_g) (2) soil moisture profile (η) (3) vegetation coverage fraction (σ_f) and (4) vegetation characteristics.

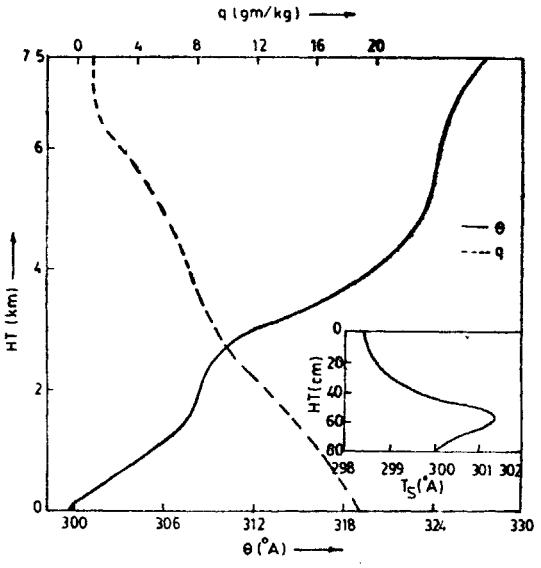

FIG 3 Initial Potential temp. (θ), specific humidity (g) soil temp (T_s) (in set fig) profiles for 1st April 1969, 00 GMT data at Port Blair.

TABLE I

Observed wind speed and direction at Port Blair
1 April 1969 00 GMT (0600) LST)

Height (m)	speed (m/s)	direction (degree) (from north)
2	0	360
500	1.5	60
1000	1	75
1500	2	90
2000	6	100
2520	6	110
3120	6	120
3700	4	105
4400	4	100
5050	7	50
6600	8	70

TABLE II

Values of soil parameters with dimensions

Soil type	η_s	ψ_s cm	K_{η_s} cm s^{-1}	b	C_t Cal cm^{-1} C^{-1}
Loamy sand (Andaman)	0.41	—9.0	0.01563	4.38	0.336

TABLE III

Values of vegetation characteristics

Emissivity	0.95
Albedo	0.15
Surface resistance r_c (s cm^{-1})	1.3
Leaf area index	$7\sigma_f$

C_g was calculated[15] at the first grid level (z_1) of the model above the surface, 25m with vegetation, by

$$C_g = (k_o/\ln (z_1 - d)/z_o)^{1/2}, \qquad ...(16)$$

where $d = 0.76\ H_c$ and $z_o = 0.08\ H_c$, where H_c is the average height of the tree canopy.[3] The relations agree with Amazon forest observations.[16] k_o is the Von Karman's constant. It was specified to be 0.35, and it was independent of atmospheric stability.

With the above data and initial conditions, two dimensional simulations were performed on a 21 × 16 grid with a minimum grid interval of 6 km near the island in the zonal direction, and a variable grid with a minimum of 2m in the vertical. Starting at the local sunrise time 0600 LST, the model equations were integrated for 24 hours using time steps of 45 seconds.

RESULTS AND DISCUSSION

The predicted atmospheric and ground surface variables for the following situations are discussed :—

Case 2S1 : flat dry island with $\eta = 0.07$

Case 2S2 : flat moist island with $\eta = 0.1$

Case 2S3 : same as 2S2 but for an island with topography.

Case 1S4 : one dimensional study $\eta = 0.1$.

Case 2V1 : same as (2S3) but for an island with vegetation cover.

The situtions in 2S1 and 2S2 consider exclusively the effects of soil moisture on the ground surface, and atmospheric variables. Simulations with two different moisture contents η were considered. These values correspond to an initial moisture content of 7 per cent and 10 per cent by volume of the soil respectively.

The hourly variations of surface temperature and surface specific humidity with different initial moisture contents are shown in Figs 4 and 5. The results showed that with drier soil ($\eta = 0.07$), higher surface temperatures were realized in comparison to wetter soil ($\eta = 0.1$). With higher initial moisture content, the surface specific humidity during the entire integration period remained higher than that with drier soil. The ground surface temperature variations were fairly symmetric about the local noon in both simulations. Considerable asymmetry was noticed in ground specific humidity variations. The gradual fall, and subsequent uniform specific humidity with drier soil, in the late afternoon hours denote an

exchange of moisture between the atmosphere and the ground as a consequence of advection. About one hour before sunset, a surface inversion formed in the atmosphere capping the region of turbulent heat transfer. This resulted in the reversal of moisture flux from the atmosphere to the ground, as shown by a rise in the ground specific humidity (Fig 5). With the advection of moisture in the simulated area, a moisture gradient between the atmosphere and the ground was established. This gradient vanished in the late afternoon, leading to a constant ground specific humidity.

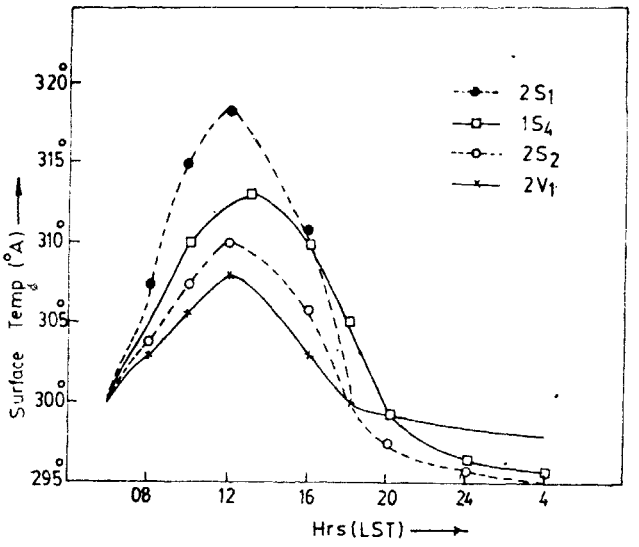

FIG 4 Model simulated hourly surface temperature (T_g) for different cases

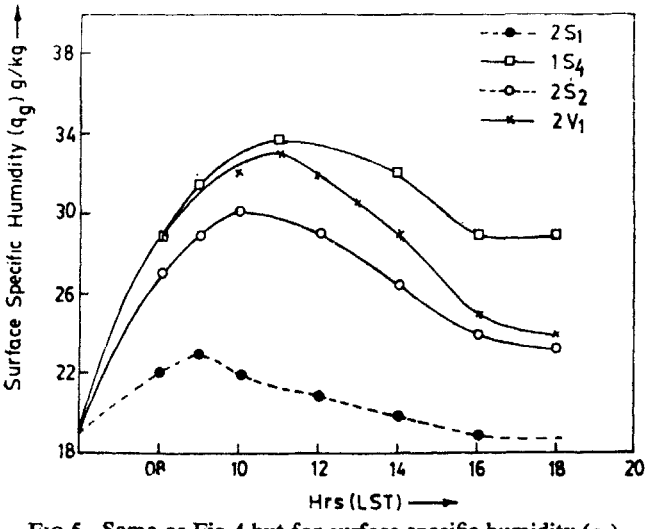

FIG 5 Same as Fig 4 but for surface specific humidity (q_g)

The calculated albedo values were in the range of 0.25 to 0.29 over drier soil ($\eta = 0.07$), while with more moist soil it ranged from 0.26 to 0.28. Rapid variations were also obtained with lower soil moisture content. A comparison of surface temperature,[2] with constant albedo and soil wetness, revealed only a small difference in heating and cooling rates at the surface. However, the maximum temperatures in both cases remained the same.

Under the combined effect of higher soil moisture and lower albedo changes, a milder temperature gradient was established between the extreme ends of the island. With $\eta = 0.1$ a temperature difference of $\sim$ 1 °C while with $\eta = .07$ a difference of $\sim$ 2 °C, was noticed between the lee and the windward ends of the island. As shown in Fig 4, generally higher surface temperatures were realized over the entire island with drier soil.

The simulated horizontal wind speeds and potential temperature profiles with variations in initial moisture contents have shown (not given here) higher temperature and larger wind speed in the boundary layer with drier soil. Correspondingly, a net increase in temperature by about 1 °C was noticed over drier soil when compared to more moist soil. As a consequence of higher warming, the PBL depth increases by about 800m, with an increase in wind speeds by $1 ms^{-1}$.

The reason for these differences become clear by comparing the magnitudes of heat fluxes. The temporal changes of sensible heat fluxes are shown in Fig 6. In this diagram, the fluxes to the atmosphere are taken to be negative. With drier soil, a greater amount of sensible heat flux (about $250 Wm^{-2}$) was transferred to the atmosphere, while the latent heat flux transfer was about $150 Wm^{-2}$. For moist soil the simulated sensible and latent heat fluxes were 150 and $380 Wm^{-2}$. A larger sensible heat transfer from dry land surface caused higher warming and large wind speeds in the PBL.

To consider advection of the simulated flow, it was necessary to compare the results of 1*D* and 2*D* simulations (2S2 and 1S4). In general 1*D* values, shown in Fig 4 through 5, have higher magnitudes, except for wind velocity, than those obtained with 2*D* simulations. In the absence of other forcing functions, such as, topography and vegetation, the reduced values are due to advection. Advection moderates the magnitudes of the atmospheric and ground variables. In the absence of pressure gradients in a 1*D* study, where the horizontal homogeneity of forcing functions was assumed, the changes in wind speed were negligible.

Effect on Sea Breeze Circulation

The sea breeze leads to a change in the direction of u, the zonal or normal component of wind to the coast line. The vertical profiles of u at 1200 LST for different situations are shown Fig 7 for $\eta = 0.1$ and $\eta = 0.07$. A temperature gradient with a larger soil moisture ($\eta = 0.1$) leads to a reduction in the magnitudes of the sea breeze when compared to drier soil. A shallow sea breeze was noticed for moist soil. Except for a slight change in the magnitudes, the above results remained unaltered even when topography was included.

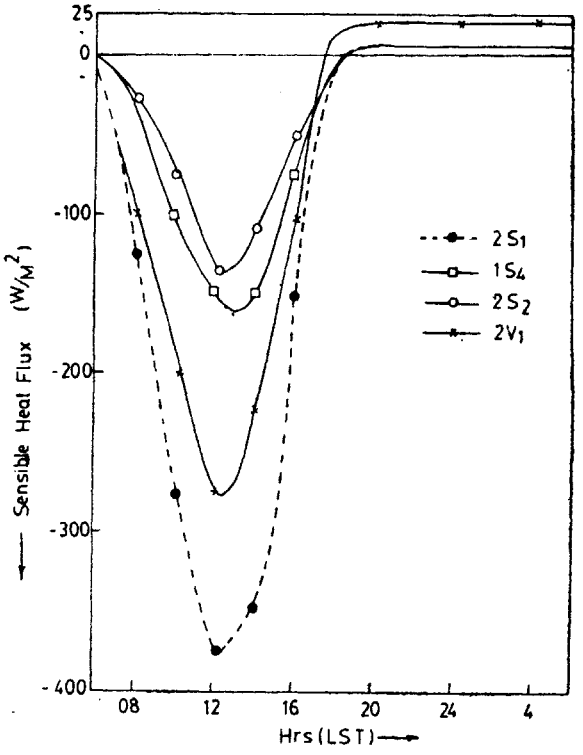

FIG 6 Diurnal variatian of sensible heat flux (w/m²). Outgoing fluxes are taken as negative.

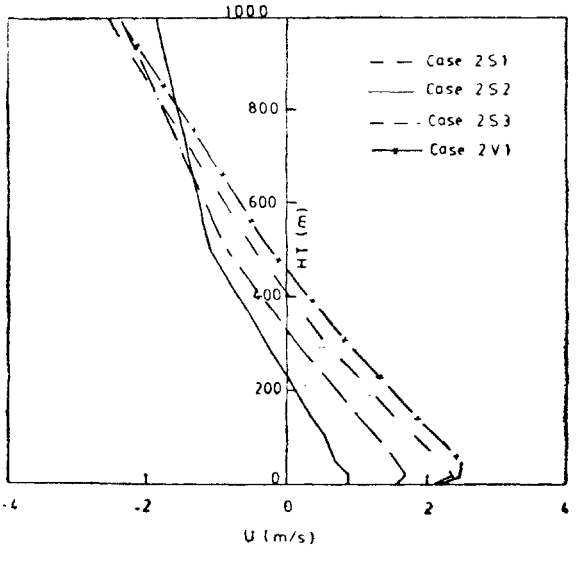

FIG 7 Vertical profiles of sea breeze (*u* component) at 1200 LST on the Lee and of island.

Influence of Vegetation

The vegetation canopy cools the ground beneath it and modifies the boundary layer climate by acting as a secondary source of heat fluxes to the atmosphere. As suggested in section 4, with vegetation canopy, the first level of the model was taken at 25m above the ground surface and σ_f was set at 0.86. The simulated values of the surface temperature, surface specific humidity, sensible heat fluxes are shown in Figs 4 through 6, with an initial soil moisture content of $\eta = 0.1$.

A comparison of surface temperature with and without vegetation shows a reduction in magnitudes with vegetation. We attribute this to the cooling (shade) effect of trees. Higher surface specific humidity with vegetation was obtained due to a decrease in the incident solar radiation at the ground, and subsequent decrease in upward moisture flux. Similar comparisons showed in increase in wind velocities and a warming of the boundary layer due to an increase in diabatic fluxes to the atmosphere by vegetation. This is shown in Fig 6. The albedo of trees is lower than the albedo of the soil. The hourly Bowen ratio (β), (the ratio between sensible and latent heat fluxes, with vegetation) during day time range from 0.7 to 0.85. This is in reasonable agreement with observations made over the Amazon forests of Brazil.

The sea breeze circulations develop with higher intensity as shown in Fig 7. The horizontal extent of inland penetration by the sea breeze also increases by about one km (not shown here). The vertical cross sections of u show that the depth of sea breeze was about 550m. A much shallower development (around 300m) obtained without vegetation as in Fig 7.

A comparison of the spatial variations of the PBL at 1400 LST, close to the time of maximum surface heating with and without vegetation but including topography (2S3 and 2V1), for $\eta = 0.1$., (As expected), due to an increased heat transfer by vegetation led to a deeper boundary layer. The PBL depth with less initial moisture ($\eta = 0.07$) was also much greater (not shown here).

The vertical velocities (W^*), developed with vegetation had greater intensities. When compared with no vegetation case (not given here), the simulated maximum positive vertical velocity of 0.25ms^{-1} was obtained over the island with vegetation compared to a weaker upward cell with a maximum W^* of 0.12ms^{-1} over bare ground. In both cases, subsiding cells developed at the both sides of an ascending cell.

In Fig 8, the model predicted horizontal wind speeds with and without vegetation are compared with observations at 25m height. As observations at 25m are not available, interpolated values were used. The results obtained with vegetation appear to be closer to observations. The deviations can be due to neglect of meridional advection in this study.

The results of our simulations show that soil moisture is the primary controlling factor in the variations of other parameters considered here. Albedo changes appear to have only secondary effects. The importance of including vegetation effects is clearly brought out in this study.

The present solutions are of an indicative nature that are valid under specified conditions. The magnitudes of simulated variables could alter depending upon the initial data. This is illustrated by Figs. 9 and 10, where the Bowen ratio is shown with different initial specifications of LAI and stomatal resistance, the two important parameters used in the present scheme.

Conclusion

The atmospheric mesoscale model with a soil and vegetation parameterisation was used to simulate the surface and atmospheric boundary layer characteristics over the Andaman Islands. A comparison with observations shows that more realistic results are obtained by including soil moisture and vegetation. Further studies should include condensation, clouds and meridional advection. This is in progress.

Acknowledgements

The authors are grateful to Professor R A Pielke for providing us a listing of his

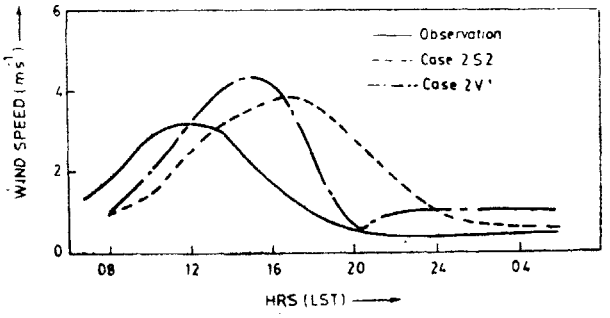

Fig 8 A comparison of horizontal wind speed (v) at 25m above the ground surface.

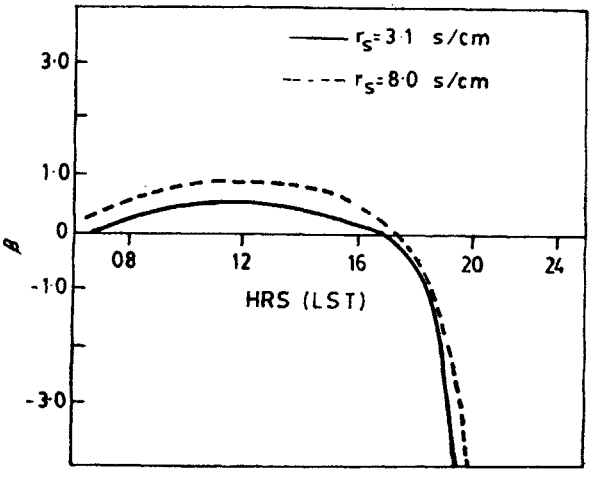

Fig 9 Hourly variation of Bowen ratio (β) for different stomatal resistance (r_s).

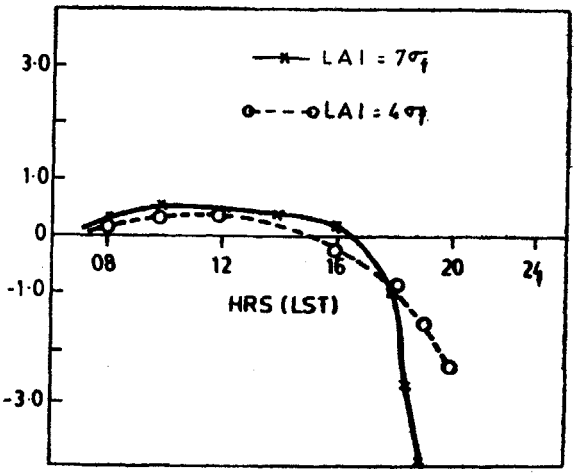

FIG 10 Same as Fig. 9, but for different Leaf Area Index (LAI).

model. The help rendered by Professor P K Das for reading the manuscript and giving useful suggestions is gratefully acknowledged. Thanks are due to Professor M P Singh, Head, C.A.S., for his keen interest and encouragement and to NIC authorities for providing necessary computing facilities.

Appendix

List of Symbols not defined in the text

ρ	—	air density
C_p	—	specific heat of air at constant pressure
c_g	—	surface drag coefficient
q_g	—	surface specific humidity
u, v	—	zonal and meridional component of wind
w^*	—	vertical velocity
u_g, v_g	—	geostrophic components of u, v
θ	—	potential temperature
q	—	specific humidity
I_1	—	horizontal extent of grid doman in x-direction
ψ_s	—	saturated moisture potential of the soil
K_{n_s}	—	saturated hydraulic conductivity
b	—	exponential constant used to calculate K_n and ψ
π	—	scaled pressure (exeners function)
ϵ_g	—	emissivity of the ground
σ	—	Stefan-Boltzman constant

REFERENCES

1 Y Mahrer and R A Pielke *Contrib Atmos Phys* **50** (1977) 98
2 S C Kar and N Ramanathan *Proc Indian Acad Sci (Earth Planet Sci)* **96** (1987) 169
3 J W Deardorff *J Geophy Res* **83** (1978) 1889

4 M C McCumber *Ph D Thesis* Univ Virginia (1980) p 255
5 T Yamada *J met Soc Japan* **60** (1982) 439
6 A J Garret *J appl Met* **22** (1983) 79
7 J F Mahfouf, E Richard and P Mascart *J Clim appl Met* **26** (1987) 1483
8 Y Mahrer and R A Pielke *Mon Weather Rev* **104** (1976) 1392
9 R A Pielke *Mesoscale Meteorological Modelling* Academic Press, Florida (1984) p 612
10 M McCumber and R A Pielke *J geophys Res* (1981) 9929
11 R Clapp and G Hornberger *Wat Resour Res* **14** (1978) 601
12 R Lee *Forest Micrometeorology* Colombia Univ Press New York (1978) 87
13 A Perrier *Land Surface Processes in Atmospheric General Circulation Model* (*Ed* P Eagleson Cambridge Univ Press (1978) 395
14 J Simpson *The Forest Atmosphere Interaction* (*Eds* B Hutchison and B Hicks) D Reidel Company (1985) 197
15 A S Thom *Q J R Met Soc* **97** (1971) 414
16 L De Abreau Sa, Y Viswanadham and A Manzo *J Theor appl Climatol* (1988) Pre-Print copy